

Original Research Article

Evaluation of a low-cost camera for agricultural applications

ABSTRACT

This study aimed to modify a webcam by replacing its near-infrared (NIR) blocking filter to a low-cost red, green and blue (RGB) filter for obtaining NIR images and to evaluate its performance in two agricultural applications. First, the sensitivity of the webcam to differentiate normalized difference vegetation index (NDVI) levels through five nitrogen (N) doses applied to the Batatais grass (*Paspalum notatum* Flugge) was verified. Second, images from maize crops were processed using different vegetation indices, and thresholding methods with the aim of determining the best method for segmenting crop canopy from the soil. Results showed that the webcam sensor was capable of detecting the effect of N doses through different NDVI values at 7 and 21 days after N application. In the second application, the use of thresholding methods, such as Otsu, Manual, and Bayes when previously processed by vegetation indices showed satisfactory accuracy (up to 73.3%) in separating the crop canopy from the soil.

Keywords: NDVI; Paspalum notatum fluegge; Otsu; segmentation.

1. INTRODUCTION

Recent developments in sensor technologies have made digital cameras more and more efficient and affordable. These systems have been widely used as a versatile remote sensing tool for many applications due to its advantages over film-based aerial photography and satellite imagery [1]. The main advantage of digital photography lies in simplified image processing [2]. Among the advantages of digital photography from these cameras are its relatively low cost, high spatial resolution and near-real-time availability of imagery for visual assessment and image processing.

Digital cameras are fitted with either a charge-coupled device (CCD) sensor or a complementary metal oxide semiconductor (CMOS) sensor that are photoconductive devices. These sensors are sensitive to near-infrared (NIR) wavelengths, however, most of these cameras are fitted with a blocking filter to this wavelength. Thus, typically these images present only the red, green, and blue (RGB) bands, which are sufficient to represent colors in the visible portion of the spectrum (400 – 700 nm), as recognized by the human vision [3]. In most cases, the digital photographs are recorded in joint photographic experts' group (JPEG) or tagged image file format (TIFF), and the RGB channels are obtained through image processing.

The use of images with RGB and NIR bands is very common in agricultural applications, especially for vegetation monitoring. Many vegetation indices, such as the normalized difference vegetation index (NDVI) [4] require spectral information in the NIR and red bands,

30 even though the RGB bands could be sufficient for some applications [5]. Since most
31 consumer-grade cameras only provide RGB bands, NIR filtering techniques can be used to
32 convert an RGB camera into a NIR camera. Moreover, it is possible to replace the blocking
33 filter by a long-pass infrared filter on standard CCD or CMOS sensors for obtaining NIR
34 images [6].

35 Over the years, numerous systems for collecting images based on cameras or webcams
36 have been developed and modified to obtain NIR information across multiple domains. Most
37 systems included analysis of the nutritional status of agricultural crops [7], disease detection
38 [8], yield estimation [9], and weed identification [10]. In addition, other authors highlight the
39 possibilities of using vegetation indices combined with segmentation techniques and texture
40 analysis for obtaining data of interest, such as crop canopy and soil [11, 12]. Furthermore,
41 these cameras can be mounted in a stationary installation [13] or onboard a light aircraft or
42 unmanned aerial vehicle, a deployment which was made possible due to its low weight [14,
43 15].

44 Given the many possibilities of using images from RGB or modified cameras to access the
45 NIR band, the use of artificial vision systems through image processing has enabled the
46 extraction of information of interest, which proves to be a great tool for application in the
47 agricultural environment. However, there are still factors, such as different ambient lighting
48 conditions, plant shading and complex background that are challenges to the success of
49 using low-cost images for agricultural applications as described in other studies [16, 17].
50 Therefore, in view of the challenge to obtain these images with good quality for solving
51 problems, the present study aimed to modify a webcam to obtaining data from the NIR band
52 and to evaluate its performance over different agricultural applications.

53 2. MATERIAL AND METHODS

54 The experiment was conducted at the Federal University of Viçosa, Viçosa Campus in Minas
55 Gerais, which is located among the coordinates: 20° 45' 14 "(S) and 42° 52' 54" (W), 649
56 meters above sea level. The image acquisition system comprised two C3 Tech model HB
57 2105 webcams that produced images in JPEG format (640x480 pixels).

58 In order to obtain NIR images, a modification was carried out in one of the webcams by
59 removing the NIR blocking filter, and adding an RGB blocking filter, which was made from
60 the magnetic material of a floppy disk (common diskette) as proposed by [18]. Thus, the
61 unmodified webcam, named in this study as RGB webcam and the modified NIR webcam
62 were tested on two different applications. First, the performance of the webcam's images to
63 differentiate NDVI values according to different N rates was verified. Second, these images
64 were processed for separating the crop canopy from the soil using different thresholding
65 algorithms.

66 In the first application, a field experiment was carried out using the Batatais grass (*Paspalum*
67 *notatum* Flugge), where a randomized block design with five treatments and five replications
68 was adopted. Treatments consisted of five nitrogen (N) doses in the form of ammonium
69 sulfate ((NH₄)₂SO₄), which corresponded to 0, 40, 80, 120 and 160 kg ha⁻¹. Plot dimensions
70 were 1_m x 1 m.

71 Furthermore, the digital images were captured with both webcams at a height of 3 m from
72 the ground. Data acquisition was performed twice with images being captured at 7 and 21
73 days after the N application. All images were geometrically corrected through the projective
74 transformation technique using the Matlab® software, where reference points were defined at

Comment [AL1]: How was the webcam installed.

75 the boundaries of each plot. Lastly, the NDVI [4] was calculated by Equation 1 for each
76 experimental plot.

$$77 \quad NDVI = \frac{nir - r}{nir + r} \quad (1)$$

78 Where: nir: near-infrared band; and r: red band.

79 In addition, the portable chlorophyll meter (SPAD-502, Konica Minolta Sensing, Tokyo,
80 Japan) was used to measure the SPAD index (SI). Thus, at the 7 and 21 days after N
81 application, 30 readings per plot were taken, where the average of all readings was
82 considered as a result. In this study, the SPAD-502 readings were assumed to be the
83 reference of chlorophyll content for the purpose of validating the sensitivity of the webcams
84 in detecting the effect of N doses over the Batatais grass.

85 In order to verify the significance of the proposed treatments, the results were submitted to
86 analysis of variance (ANOVA) through the F-test. Lastly, regression models were adjusted to
87 assess treatment effects on results of the SPAD index readings and NDVI values. All
88 analyses were carried out using the ASSISTAT, version 7.7 free software [19].

89 In the second application, the RGB images were used for the ability to differentiate crop
90 canopy from soil under different growing conditions. There were 30 images captured for this
91 study and all of it belonged to maize crops at the V4 vegetative stage (four expanded
92 leaves), which were grown under different soil cover conditions, such as conventional
93 planting system, and no-tillage system with coffee husk and straw residue.

94 The digital images were captured at a height of 1.5 m from the ground and then stored as
95 24-bit colour images with resolutions of 640 × 480 pixels saved in RGB colour space in the
96 JPEG format. Then, to discriminate between the object of interest (plant) and background
97 (soil), algorithms were developed using different thresholding methods, such as Otsu [20],
98 Manual threshold selection, and Bayes [21].

99 Initially, two methods were used to accentuate the green color of plants in RGB images.
100 First, in the absolute green method, the pixel color distance (PCD) value was obtained
101 through the euclidean distance (ED) calculation using normalized values from the red and
102 green bands of each pixel, as shown in Equation 2 [22].

$$103 \quad PCD = \sqrt{pixel(r^2) + [pixel(g) - 1]^2} \quad (2)$$

104
105 Where: r: pixel value from the red band; and g: pixel value from the green band.

106 Second, the excess green normalized index (ExG) was obtained as it is shown in Equation 3
107 [23].

$$108 \quad ExG = \frac{2 \times g - r - b}{r + g + b} \quad (3)$$

109 Where: g: pixel value from the green band; r: pixel value from the red band; and b: pixel
110 value from the blue band.

111 Subsequently, the Otsu, Manual, and Bayes methods were applied to each image. As a
112 result, all images showed some noise, which was removed by using a median filter with a

Comment [AL2]: Give a reference to the literature.

Comment [AL3]: Have you checked the assumptions of using ANOVA? Normal distribution, equality of variance?

Comment [AL4]: Where? I did not find the results.

113 | 3_m ~~x~~ 3_m window size. Moreover, the ground truth segmentation model for comparison of
114 | the three algorithms was developed from the K-means method.

115 | Generally, this method can be employed in different areas including image processing,
116 | where it can be used as a thresholding method based on data clustering. This method
117 | partitions n pixels into k clusters, where k is an integer value that holds $k < n$. k-means
118 | algorithm classifies pixels in an image into k number of clusters according to some similarity
119 | feature, such as the grey level intensity of pixels, and distance of pixel intensities from
120 | centroid pixel intensity [24].

Comment [AL5]: Dot?

121 | The algorithm is based on six steps:

- 122 | 1. Selection of k clusters (k is a user defined parameter);
- 123 | 2. Calculation of the number of image pixels N;
- 124 | 3. Selection of k initial pixel intensity centroids μ_j ;
- 125 | 4. Calculation of distances D_{ij} between pixel x_i and each centroid μ_j as given in Equation 4.

$$126 | \quad \quad \quad D_{ij} = (x_i - \mu_j)^2 \quad \quad \quad (4)$$

128 | Where: $i = 1 \div N$; and $j = 1 \div k$.

129 | Particular pixel x_i is then classified to cluster c_j to which centroid it has the smallest distance.

Comment [AL6]: all variables in italics, except for Greek letters

- 131 | 5. Recalculation of centroid positions μ_j as a mean value of all pixel intensities, which
132 | belong to cluster c_j as shown in Equation 5.

$$133 | \quad \quad \quad \mu_j = \frac{1}{l_j} * \sum_{i=1}^{l_j} x_i \quad \quad \quad (5)$$

134 | Where: l_j is the number of pixels that belong to cluster c_j .

- 135 | 6. Steps (4) and (5) are repeated until classification of the image pixels does not change.

136 | In this study, the value of k (number of clusters) was defined as two, where the first
137 | represented the crop canopy and second the soil. Then, in order to validate the performance
138 | of each thresholding method, the accuracy index, proposed by [25] was computed using
139 | Equation 6.

$$140 | \quad \quad \quad Accuracy = 100 \times \frac{A \cap B}{A \cup B} \quad \quad \quad (6)$$

141 | Where: A: represents the set of pixels in the ground truth image that is marked as crop
142 | canopy; and; B: represents the set of pixels in the segmentation that is marked as crop
143 | canopy.

144 | This measure of accuracy determines how closely the segmentation matches the ground
145 | truth, with 100% indicating an exact match and perfect segmentation. Thus, to verify the
146 | significance of the proposed methods, the accuracy means were compared by the Students t
147 | test at a 5-% significance level ($\alpha < 0.05$).

Comment [AL7]: Have the tests been carried out in comparable atmospheric conditions?

148 **3. RESULTS AND DISCUSSION**

149 **3.1 Application 1**

150 Average values of the SI and NDVI as a function of the nitrogen doses, as well as its
 151 respective coefficient of variation (CV), are shown in Table 1. It can be observed that CV
 152 values for NDVI index were higher than to SI values at 7 and 21 days, which may be justified
 153 by the low uniformity of the Batatais grass on the study area. Furthermore, the fact that
 154 SPAD readings are done by direct contact with the leaf surface might have decreased its
 155 CV. In addition, its higher number of readings per plot also contributes to decrease CV
 156 values, which is not done in the NDVI calculation, since only one RGB, and NIR images are
 157 used per plot to obtain the index.

Comment [AL8]: But is this a statistically significant difference? Where test?

158 **Table 1. Descriptive statistics of the SI (SPAD index) and NDVI (normalized difference**
 159 **vegetation index) at 7 and 21 days after N application.**

Time Days	N rates (kg ha ⁻¹)					CV (%)
	0	40	80	120	160	
SI (SPAD-502)						
7	40.22	43.17	43.20	44.95	47.00	3,67
21	37.95	44.92	48.12	45.82	46.95	6.55
NDVI (webcam)						
7	0.19	0.23	0.27	0.31	0.33	26,4
21	0,23	0.25	0.26	0.22	0.39	17.9

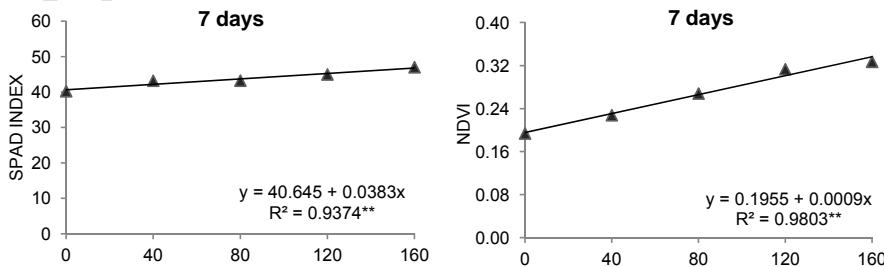
Comment [AL9]: Everywhere, change the decimal separator to a dot instead of a comma.

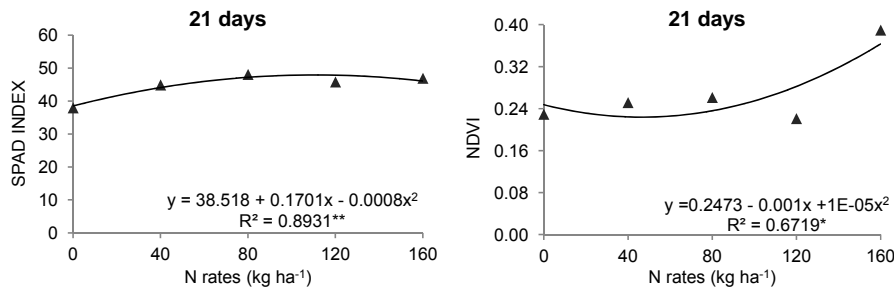
160 CV: Coefficient of variation

161 Even showing sensitivity to the applied N rates, NDVI results from both dates (7 and 21
 162 days) were relatively low, which might be associated with low uniformity of the vegetation,
 163 and absence of radiometric calibration. [26] highlights that using a reference panel for
 164 standardization or the inclusion of a gray Spectralon (or other diffuse reflectors) panel within
 165 the field of view of the webcam would potentially be of value for calibration under changing
 166 illumination conditions (e.g. cloudy vs. sunny days). Thus, a radiometric calibration could
 167 increase the sensitivity of the webcam, which would result in higher NDVI values and lower
 168 weather interference. However, the results obtained here suggest that even without this
 169 calibration, the webcam was still capable of detecting differences among treatments.

170 The regression analyses carried out to access the effect of nitrogen doses on SI and NDVI
 171 values at 7 and 21 day after N application showed a linear (7 days) and quadratic (21 days)
 172 response for both indices. Moreover, both indices were significant at 1% probability with a
 173 coefficient of determination (R²) of 0.93 (SI), and 0.98 (NDVI), respectively. In Figure 1 it is
 174 possible to observe the linear increase of the SI and NDVI values as the N doses increases
 175 at 7 days after the fertilization.

Comment [AL10]: Have you checked the statistical significance of regression coefficients, eg is 1E-05 at x² a statistically significant value? Provide Student-t or p-value test proof for this factor. R² is not enough.





177

178 **Fig 1. SPAD Index (SI) and NDVI index as a function of topdressing nitrogen doses.**

179 When observing the SI values at 21 days (Figure 1), a linear increase in its values is also
 180 observed up to the dose of 80 kg ha⁻¹ of N. However, from the 120 kg ha⁻¹ of N, SI values
 181 showed a decrease, which demonstrates a quadratic response to different N doses.
 182 Similarly, NDVI values showed a linear increase up to 80 kg ha⁻¹ of N. Although, when
 183 looking at 120 and 160 kg. ha⁻¹ N doses, NDVI response showed a high variation for both
 184 treatments, which resulted in low correlation ($R^2 = 0.67$). Even though there was a high
 185 variation in response to these treatments, SI and NDVI values at 21 days were also
 186 significant at 1%, and 5% probability, respectively.

187 In general, this quadratic response for both indices at 21 days indicates that, in this range,
 188 increasing the nutrient concentration (nitrogen) would not reflect on grass growth, and it
 189 represents the plant luxury consumption. According to [27], the luxury consumption is
 190 defined as the N storage in the vacuole instead of its participation in the chlorophyll
 191 molecule. The same authors also point out that, excessive consumption is not always
 192 undesirable since it allows plants to accumulate nutrients when its availability is high. In this
 193 case, a gradual release is performed by the plant, when the absorption is insufficient to
 194 support its growth.

195 Results obtained in this study showed that the webcam sensor was capable of detecting the
 196 effect of N doses over the Batatais grass for both dates, at 7 and 21 days after N application.
 197 The SPAD-502 used here as a reference method presented better results, which was
 198 expected due to its higher sensitivity and correlation with the leaf chlorophyll content.

199 Compared to other low-cost, sensor-based methods for monitoring crops phenology, such as
 200 radiometric instruments based on LED sensors [28], or light emitting diodes [29], a clear
 201 advantage of using webcams is that it can yield images with good spatial resolution. This
 202 enables tracking the phenology of different crops by breaking the image into different regions
 203 of interest (e.g., crops and weeds) [26]. On the other hand, there is no doubt that higher-
 204 quality spectral imaging could, potentially, be obtained from existing, commercially available
 205 multispectral cameras. However, for budget-limited observational and experimental studies,
 206 the system proposed here may represent an acceptable compromise, given its low cost and
 207 promising performance.

208 3.2 Application 2

209 Initially, performance analyses of segmentation algorithms were based on visual analysis by
 210 comparing the proposed methods to the reference binary image. Then, the accuracy index
 211 (equation 6) was used for comparing each result with that obtained through the K-means. In
 212 general, segmentation methods when combined with the ExG index showed higher accuracy

Comment [AL11]: Why? Can you explain if it is a measurement error, e.g. related to change in weather conditions.

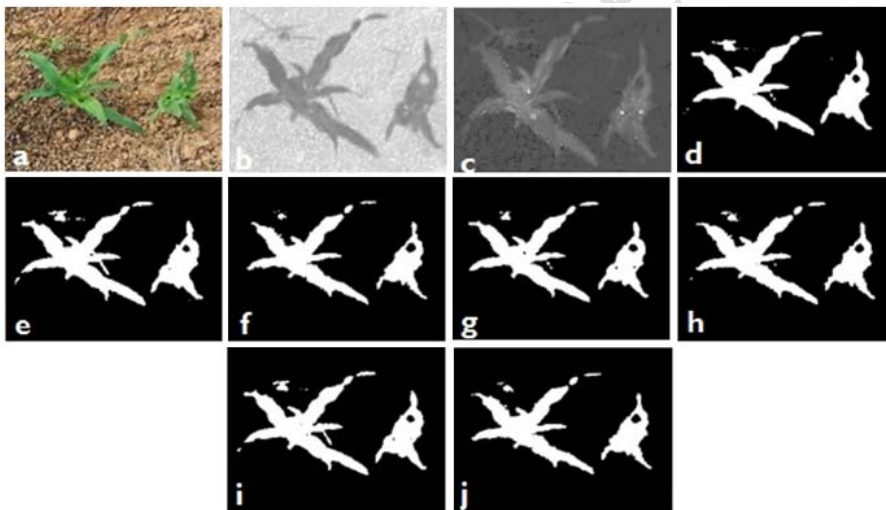
Comment [AL12]: Are you sure about that?

Comment [AL13]: Is this statement not too sharp. It's better to add that it can be.

213 results than those methods preceded by the euclidean distance (ED). Moreover, the highest
 214 overall mean accuracy (80.3%) was obtained using the Otsu method preceded by ExG
 215 index. On the other hand, the lowest accuracy mean was observed using the Manual
 216 method with the ED index (73.3%).

217 These results corroborate with [30], which observed that images segmented by the Otsu with
 218 the ExG index showed 88% accuracy when compared to other indices using RGB bands. In
 219 another study [31], these authors when using the Otsu method preceded by different indices,
 220 such as ExG, ExR (excess of red), and another index based on the CIE L^*a^*b color space
 221 obtained accuracies of 74%, 77.2%, and 62%, respectively. This demonstrates that the
 222 contrast provided by vegetation indices is of great use to highlight the crop canopy from the
 223 soil, and could yield in high accuracy segmentation.

224 When analyzing the accuracy of each image, the highest values were observed for the
 225 Manual and Otsu method when preceded by the ED index, which resulted in 95.9% of
 226 accuracy for both methods. According to [22], the ED method is based on the search for
 227 homology among plants, where after obtaining the spectral energy of plant content; its
 228 similarity is verified through the Euclidean distance measurement. Figure 2 shows examples
 229 of resulting images from the proposed segmentation algorithms.



230
 231 **Fig 2. Images processed by the proposed segmentation algorithms. (a) RGB image,**
 232 **(b) Euclidean distance, (c) ExG index, (d) K-means, (e) Bayes with ED, (f) Bayes with**
 233 **ExG, (g) Manual with ED, (h) Manual with ExG, (i) Otsu with ED, and (j) Otsu with ED.**

Comment [AL14]: The picture is not very good.

234 In order to determine the most accurate method, the data set was submitted to the Student t-
 235 test at 5% significance level. Results from the ANOVA showed that statistically, there was no
 236 difference in performance among the proposed methods when compared to each other.
 237 Although, the highest CV values were obtained through Bayes (34.72%), and Otsu methods
 238 (33.28%), when preceded by the ED index as it is shown in Table 2.

239 **Table 2. Accuracy results from the proposed segmentation algorithms.**

Methods	Accuracy (%)				
	Max	Min	SD	CV	Mean

Otsu + ED	95.9	32.0	25.65	33.28	77.1
Otsu + ExG	90.9	61.6	9.09	11.33	80.3
Manual + ED	95.9	32.0	23.43	31.99	73.3
Manual ExG	93.5	55.9	13.05	17.12	76.2
Bayes + ED	93.7	22.5	26.15	34.72	75.3
Bayes + ExG	90.9	61.6	16.11	21.19	76.0

240 Max: maximum; Min: minimal; SD: Standard deviation; CV: coefficient of variation. ED: Euclidean
241 distance; ExG: Excess of green

242 These results can be justified by the adverse illumination conditions during the image
243 acquisition period, which resulted in erroneous segmentation due to shaded areas in
244 images. Thus, the Otsu, manual, and Bayes segmentation methods presented satisfactory
245 accuracy (up to 73.3%) for separating crop canopy from the soil when preceded by the ExG
246 and ED indices. Even though a satisfying performance has been achieved, there are still
247 factors, such as the lighting conditions, plant shading and complex background that are
248 challenges to the success of segmentation.

249 Thus, the application of low-cost consumer cameras for process control as an element of
250 precision farming could save fertilizer, pesticides, machine time, and labor force. Although
251 research activities on this topic have increased over the years, high camera prices still reflect
252 on low adaptation to applications in all fields of agriculture. Smart cameras adapted to
253 agricultural applications can overcome this drawback.

254 4. CONCLUSION

255 The webcam sensor was capable of detecting the effect of nitrogen doses over the Batatais
256 grass through different NDVI values at 7 and 21 days after N application. Regarding the use
257 of webcam images in agricultural applications through thresholding methods, it was possible
258 to observe that the segmentation process over RGB images becomes challenging due to
259 non-uniform illumination conditions, and complex image background. Thus, the use of
260 thresholding methods, such as Otsu, Manual, and Bayes when previously processed by the
261 ExG and ED indices can satisfactorily separate the crop canopy from the soil. As a
262 recommendation for future studies, both images (NIR and RGB) can be used to calculate
263 vegetation indexes to perform studies on phenology or plant's nutritional status. Also, the
264 RGB images can be processed using segmentation algorithms to quantify plant diseases or
265 leaves damaged by pests in crops.

266 COMPETING INTERESTS

267 Authors have declared that no competing interests exist.

268 AUTHORS' CONTRIBUTIONS

269 This work was carried out in collaboration between all authors. All authors read and
270 approved the final manuscript.

271 REFERENCES

- 272 1. Yang C, Westbrook JK., Suh CPC, Martin DE, Hoffmann WC, Lan Y, & Goolsby JA.
273 2014. An airborne multispectral imaging system based on two consumer-grade
274 cameras for agricultural remote sensing. Remote Sensing, 6(6), 5257-5278. DOI:
275 <https://doi.org/10.3390/rs6065257>.
276

- 277
278
279
280
281
282
283
284
285
286
287
288
289
290
291
292
293
294
295
296
297
298
299
300
301
302
303
304
305
306
307
308
309
310
311
312
313
314
315
316
317
318
319
320
321
322
323
324
325
326
327
328
2. Lebourgeois V, Bégué A, Labbé S, Mallavan B, Prévot L, & Roux B. 2008. Can commercial digital cameras be used as multispectral sensors? A crop monitoring test. *Sensors*, 8(11), 7300-7322. DOI: <https://doi.org/10.3390/s8117300>.
 3. Sonnentag O, Hufkens, K, Teshera-Sterne C, Young AM, Friedl M, Braswell BH, Milliman T, O'keefe J, & Richardson AD. 2012. Digital repeat photography for phenological research in forest ecosystems. *Agricultural and Forest Meteorology*, 152(1), 159–177. DOI: <https://doi.org/10.1016/j.agrformet.2011.09.009>.
 4. Rouse JW, Haas Jr. RH, Schell JA, & Deering DW. 1974. Monitoring vegetation systems in the Great Plains with ERTS, NASA SP-351. Third ERTS-1 Symposium, Vol. 1, pp. 309 – 317, NASA, Washington, DC.
 5. Nijland W, De Jong R, De Jong SM, Wulder MA, Bater CW, & Coops NC. 2014. Monitoring plant condition and phenology using infrared sensitive consumer grade digital cameras. *Agricultural and Forest Meteorology*, 184(1), 98-106. DOI: <https://doi.org/10.1016/j.agrformet.2013.09.007>.
 6. Rabatel G, Gorretta N, & Labbé N. 2014. Getting simultaneous red and near-infrared band data from a single digital camera for plant monitoring applications: Theoretical and practical study. *Biosystems Engineering*, 117(1), 2–14. DOI: <https://doi.org/10.1016/j.biosystemseng.2013.06.008>.
 7. Jia B, He H, Ma F, Diao M, Jiang G, Zheng Z, Cui J, & Fan H. 2014. Use of a digital camera to monitor the growth and nitrogen status of cotton. *The Scientific World Journal*, 2014(1), 1-12. DOI: <http://sci-hub.tw/10.1155/2014/602647>.
 8. Castro A I, Ehsani R, Ploetz RC, Crane JH, & Buchanon S. 2015. Detection of laurel wilt disease in avocado using low altitude aerial imaging. *PLoS one*, 10(4), 1-13. DOI: <https://doi.org/10.1371/journal.pone.0124642>.
 9. Stroppiana D, Migliazzi M, Chiarabini V, Crema A, Musanti M, Franchino C, & Villa P. 2015. Rice yield estimation using multispectral data from UAV: A preliminary experiment in northern Italy. In *Geoscience and Remote Sensing Symposium (IGARSS), IEEE International* (pp. 4664-4667). DOI: <https://doi.org/10.1109/IGARSS.2015.7326869>.
 10. Romeo J, Guerrero JM, Montalvo M, Emmi L, Guijarro M, Gonzalez-De-Santos P, & Pajares G. 2013. Camera sensor arrangement for crop/weed detection accuracy in agronomic images. *Sensors*, 13(4), 4348-4366. DOI: <http://sci-hub.tw/10.3390/s130404348>.
 11. Montalvo M, Guerrero JM, Romeo J, Emmi L, Guijarro M, & Pajares G. 2013. Automatic expert system for weeds/crops identification in images from maize fields. *Expert Systems with Applications*, 40(1), 75-82. DOI: <https://doi.org/10.1016/j.eswa.2012.07.034>.
 12. Torres-Sánchez J, López-Granados F, & Peña M. 2015. An automatic object-based method for optimal thresholding in UAV images: Application for vegetation detection in herbaceous crops. *Computers and Electronics in Agriculture*, 114(6), 43-52. DOI: <https://doi.org/10.1016/j.compag.2015.03.019>.

Formatted: Polish (Poland)

- 329 | 13. Sakamoto T, Shibayama M, Kimura A, & Takada E. 2011. Assessment of digital
330 camera-derived vegetation indices in quantitative monitoring of seasonal rice
331 growth. ISPRS Journal of Photogrammetry and Remote Sensing, 66(6), 872-882.
332 DOI: <https://doi.org/10.1016/j.isprsjprs.2011.08.005>.
333
- 334 14. Caturegli L, Corniglia M, Gaetani M, Grossi N, Magni S, Migliazzi M, Angelini L,
335 Mazzoncini, M, Silvestri N, Fontanelli M, Raffaelli M, Peruzzi A, & Volterrani M.
336 2016. Unmanned aerial vehicle to estimate nitrogen status of turfgrasses. PloS one,
337 11(6), 1-13. DOI:
338 <https://journals.plos.org/plosone/article?id=10.1371/journal.pone.0158268>.
339
- 340 15. Levin N, Ben-Dor E, & Singer A. 2005. A digital camera as a tool to measure colour
341 indices and related properties of sandy soils in semiarid environments. International
342 Journal of Remote Sensing, 26(24), 5475-5492. DOI:
343 <https://doi.org/10.1080/01431160500099444>.
344
- 345 16. Vesali F, Omid M, Kaleita A, & Mobli H. 2015. Development of an android app to
346 estimate chlorophyll content of corn leaves based on contact imaging. Computers
347 and Electronics in Agriculture, 116, 211-220. DOI:
348 <https://doi.org/10.1016/j.compag.2015.06.012>.
349
- 350 17. Aureliano Netto AF, Martins RN, Aquino de Souza GS, Araujo GDM, Hatum de
351 Almeida SL, & Capelini VA. 2018. Segmentation of RGB images using different
352 vegetation indices and thresholding methods. NATIVA, 6 (4), 389-394. DOI: DOI:
353 <http://dx.doi.org/10.31413/nativa.v6i4.5405>
354
- 355 18. Micha DN, Penello G, Kawabata RMS, & Camarott T. 2011. Vendo o invisível.
356 Experimentos de visualização do infravermelho feitos com materiais simples e de
357 baixo custo. Revista Brasileira de Ensino de Física, 33(1), 1501,2011. DOI:
358 <http://sci-hub.tw/10.1590/S1806-11172011000100015>.
359
- 360 19. Silva FAS, & Azevedo CAV. 2016. The Assistat Software Version 7.7 and its use in
361 the analysis of experimental data. African Journal of Agricultural Research, 11(39),
362 3733-3740. DOI: <https://doi.org/10.5897/AJAR2016.11522>.
363
- 364 20. Otsu N. 1979. A threshold selection method from gray-level histogram. IEEE
365 Transactions on System Man Cybernetics, 9(1), 62-66. DOI:
366 <https://doi.org/10.1109/TSMC.1979.4310076>.
367
- 368 21. Gonzales RC, & Woods RE. 1992. Digital image processing (vol.2). Addison-Wesley
369 Publishing Company.
370
- 371 22. Nejati H, Azimifar Z, & Zamani M. 2008. Using fast fourier transform for weed
372 detection in corn fields. In *Systems, Man and Cybernetics. IEEE International
373 Conference on* (pp. 1215-1219). DOI: <https://doi.org/10.1109/ICSMC.2008.4811448>.
374
- 375 23. Woebbecke DM, Meyer G.E., Von Garden K, Mortensen DA. 1995. Color indices for
376 weed identification under various soil, residue and lighting conditions. Transactions
377 of the ASAE 38, 259-269. DOI: <http://sci-hub.tw/10.13031/2013.27838>.
378
- 379 24. Dass R, Priyanka, Devi S. 2012. Image Segmentation Techniques. International
380 Journal of Electronics & Communication Technology, 3(1), 1-5.

381
382
383
384
385
386
387
388
389
390
391
392
393
394
395
396
397
398
399
400
401
402
403
404
405
406
407
408
409
410
411
412
413
414

25. Coy A, Rankine D, Taylor M, Nielsen DC, & Cohen J. 2016. Increasing the accuracy and automation of fractional vegetation cover estimation from digital photographs. *Remote Sensing*, 8(7), 474-488. DOI: <https://doi.org/10.3390/rs8070474>.
26. Petach AR, Toomey M, Aubrecht DM, & Richardson AD. 2014. Monitoring vegetation phenology using an infrared-enabled security camera. *Agricultural and Forest Meteorology*, 195(9), 143-151. DOI: <https://doi.org/10.1016/j.agrformet.2014.05.008>.
27. Baesso MM, de Carvalho Pinto FDA, de Queiroz D, Santos NT, & de Souza Carneiro JE. 2013. Avaliação da deficiência de nitrogênio no feijoeiro usando um medidor portátil de clorofila. *Engenharia na Agricultura*, 21(2), 122-128. DOI: <https://doi.org/10.13083/reveng.v21i2.318>.
28. Ryu Y, Lee G, Jeon S, Song Y, & Kimm H. 2014. Monitoring multi-layer canopy spring phenology of temperate deciduous and evergreen forests using low-cost spectral sensors. *Remote Sensing of Environment*, 149(6), 227-238. DOI: <http://sci-hub.tw/10.1016%2Fj.rse.2014.04.015>.
29. Ryu Y, Baldocchi DD, Verfaillie J, Ma S, Falk M, Ruiz-Mercado I, Hehn T, & Sonnentag O. 2010. Testing the performance of a novel spectral reflectance sensor, built with light emitting diodes (LEDs), to monitor ecosystem metabolism, structure and function. *Agricultural and Forest Meteorology*, 150(12), 1597- 1606. DOI: <https://doi.org/10.1016/j.agrformet.2010.08.009>.
30. Hamuda E, Glavin M, & Jones E. 2016. A survey of image processing techniques for plant extraction and segmentation in the field. *Computers and Electronics in Agriculture*, 125(7), 184-199. DOI: <https://doi.org/10.1016/j.compag.2016.04.024>.
31. Bai X, Cao Z, Wang Y, Yu Z, Hu Z, Zhang X, & Li C. 2014. Vegetation segmentation robust to illumination variations based on clustering and morphology modelling. *Biosystems engineering*, 125(9), 80-97. DOI: <https://doi.org/10.1016/j.biosystemseng.2014.06.015>.

Formatted: Polish (Poland)